

CAPACITY SCALING IN AIRBORNE COMMUNICATION NETWORKS BASED ON AIR TRAFFIC SCENARIO MODELING

K.-D. Bächter¹, N. Randt², and A. Sizmann¹,

¹Bauhaus Luftfahrt e.V., Lyonel-Feininger-Str. 28, 80807 Munich, Germany

²Lehrstuhl für Luftfahrtsysteme, Boltzmannstr. 15, 85748 Garching near Munich, Germany

Summary

The growing demand for aeronautical telecommunication capacity presents a difficult challenge. Airborne networking represents an approach that promises large data transmission capacity over large distances. The concept has been evaluated with regard to aspects like connectivity, traffic load distribution, packet queuing and time delay. In a network in which various aircraft act as cross-connect for the larger network, however, the aggregated data traffic may necessitate photonic “backbone” links to be able to handle future internet traffic loads. The objective of this work is to evaluate the scaling properties of communication link requirements, i.e., the capacity and range, with respect to time-varying aircraft density. The analysis of this paper is based on a scenario-based model of the North Atlantic air traffic, using a global flight schedule database, and results are presented for the years 2008 (“status quo”), 2020 and 2035.

1. MOTIVATION

The growing demand for aeronautical telecommunication capacity presents a difficult challenge with regard to physical, technical, as well as regulatory boundary conditions. Apart from traditional air traffic control related aeronautical telecommunication services, novel capacity requirements arise for example due to the advent of remotely piloted vehicles. Moreover, aeronautical passenger communication represents a major driver for telecommunication capacity in commercial air transport. Airborne networking represents an approach that promises the transfer of large amounts of data over large distances at high rates. In this concept, aircraft form ad hoc networks using large capacity, directive communication links. The concept has been evaluated with regard to aspects like connectivity, path length, traffic load distribution [1], packet queuing and time delay [2] within the context of the European NewSky project for a radio frequency communication network. In a network architecture in which various aircraft act as cross-connect for the larger network, however, the aggregated data traffic may necessitate photonic “backbone” links to be able to handle future internet traffic loads [3].

In our previous work [3], a network concept was proposed that follows a hybrid approach. In this concept, high-rate directive links based on photonic technology are used to interconnect aircraft to form a backbone network of large capacity. Directive radio-frequency technology is used as a short-range access technology for less-capable aircraft with lower capacity requirements, which do not participate in the backbone. In this way, a large-capacity network could be realized with a low interference potential to other radio-frequency applications. Furthermore, High Altitude Platforms (HAPs) would serve as portals to the terrestrial internet, exploiting path-diversity as a weather mitigation strategy.

This work is meant to lay a foundation for the evaluation of such a network with future requirements in mind. The objective is to investigate the scaling properties of communication link requirements, i.e., the capacity and range, with respect to time-varying aircraft density as function of year.

The analysis of this paper is based on a model of the North Atlantic air traffic, using a global flight schedule database. The model is able to compute the time-dependent regional air traffic, including number, position and types of operating aircraft. This information allows the determination of aggregated aeronautical passenger communication capacity requirements as a function of the statistical user count, exploiting a user-based internet traffic model. The model incorporates flight schedule information of the year 2008 to simulate the status quo. An enhanced model is introduced which integrates potential air traffic situations to account for future perspectives of airborne communication. A scenario-based approach is applied here, which is an adequate method for the definition of comprehensive future situations [4]. In this paper, exemplary results of a scenario extrapolation for the years 2020 and 2035 are presented.

One finding indicates that, while low aircraft densities reduce the amount of networking opportunities due to increased mean link length, the communication capacity requirements are also reduced. Likewise, large aircraft densities offer increased networking opportunities at short distances, but also require larger communication capacities. This interrelation is favorable as the channel capacity in wireless communications increases for shorter distances. In principle, this opens up novel opportunities for airborne networks, for example by exploiting rate-adaptive technology for large-capacity backbone links. Moreover, the forecasted bitrate capacities generated by the model give an indication of future communication link requirements.

1.1. Airborne Telecommunication Network

The envisioned airborne telecommunications network features a hybrid architecture which is based on photonic links for large backbone capacity, whereas RF-technology is used for short-distance links with lower capacity. The concept is much like terrestrial cellular network architectures for mobile services, where mainly fiber-optic cables are employed for backhaul, but also directive high-frequency GHz-links. The dynamics of the airborne network, however, requires ad hoc networking capability which differs from fixed-infrastructure networks with mobile

end users. In case of the airborne network, backbone aircraft act as distribution nodes for RF-enabled aircraft, and have add-drop capabilities for through-traffic. The passenger is the end user in this scenario, using for example GSM or WLAN standards for in-cabin connectivity, or future technologies like visible-light transmission systems [5].

In order to gain access to the terrestrial internet, nodes for air-to-ground routing are needed, and we envision High Altitude Platforms (HAPs) as enablers for this task. A network of HAPs could ensure sufficient redundancy for weather mitigation by spatial diversity of platforms and ground stations. Simple realizations could be modified weather balloons, but solar-electric aircraft are a promising alternative. Due to size, weight and power limitations on such aircraft, photonic technologies are the preferred choice also for this application.

1.2. Prerequisites for Network Assessment

In order to assess the potentials of the hybrid RF-photonic aeronautical network architecture, a number of prerequisites must be understood.

A first approach to qualify and quantify the requirements and technological limitations was presented in [3]. The per-aircraft capacity demand is determined mainly by the on-board end-user behavior and depends on the type and numbers of mobile devices considered, and the usage statistics to a large degree. In a first approach to generate a finer-grained model for capacity demand than what was presented in [3], the ETSI model applied in [6] was adapted and is used for the status quo and future scenario modeling, considering web traffic growth.

From a technological perspective, very high bandwidth wireless communication depends on directive, and thus line-of-sight links. Our model is based on photonic infrared links, which have very high directivity, in order to achieve ultimate bandwidth capacity and range in the backbone network. For short range access of individual aircraft to the backbone with small interference potential, RF-technology with moderate power requirements and highly directive beam-forming antennas is envisioned. Photonic links are essentially blocked by clouds and fog and to a lesser degree by precipitation. The atmosphere itself in clear-air conditions attenuates radiation by molecular and aerosol scattering and absorption. Moreover, clear-air turbulence has a detrimental effect on systems exploiting visible or infrared light. Atmospheric ray-tracing [7] predicts a geometric limitation of about 975 km for an air-to-air link at a typical cruise altitude of 36 kft. From aircraft to HAP at 80 kft, the ultimate distance is 1240 km. Assuming a cloud altitude of 26 kft, the maximum air-to-air range is 520 km, and the maximum air-to-HAP range is 900 km. For energy transmission considering atmospheric extinction, turbulence induced scattering and free-space loss, modeling also shows that 500 km is a feasible range limitation for air-to-air links at 36 kft [8] (in this case a geometric model was used to calculate altitude-dependent atmospheric extinction, as opposed to more complex but more realistic ray-tracing).

In the following, it is assumed that the ray-tracing results with a cloud coverage of 26 kft pose hard limits on communication range. From the perspective of practicality, we assumed that few photonic terminals are available on individual aircraft for backbone communication and the network was modelled accordingly.

2. AIR TRAFFIC MODELING APPROACH

2.1. General Requirements and Constraints

In this section, we depict the major requirements and constraints that the air traffic model has to meet.

2.1.1. Project Mission

Modeling air traffic movements and densities can be motivated by several reasons: Gordon et al. [9] have built a model of air traffic movements with the goal to find the optimum structure of an air route network as a function of the number of operating aircraft in order to minimize traffic delay. Matsumoto [10] has created a model to simulate passenger and cargo flows and to identify major air traffic corridors in order to gain an understanding about the required future handling capacities of major hub airports. Salaün et al. [11] have elaborated a model that is able to calculate air traffic densities using probabilistic methods to identify potentially dangerous airspace areas with regard to aircraft collision.

The purpose of the air traffic model used for the study presented here is to calculate local air traffic densities with a certain degree of geographical and chronological resolution in order to identify design requirements for an airborne communication network, both for a representative present situation as well as for future scenarios.

2.1.2. Input Data Requirements

It is trivial to state that the air traffic model is required to simulate reality as precisely as possible. This, however, presents a major problem with regard to the required input data: in the case of simulating the present air traffic situation, the best modeling results can only be obtained if data of actual flight movements is available (i.e., trajectory records of real flight operations containing position information of each operating aircraft at every moment within a predefined period of time). This kind of data has not been available for this study though. Thus, a model was developed that is solely based on a flight schedules database to simulate the status quo traffic situation.

Simulating the long-term future air traffic posed another issue in this context since corresponding flight schedule information is not available. Consequently, future-related traffic data have been generated by developing multiple, alternative future scenarios in order to cover a wide spectrum of potential future situations.

2.1.3. Output Data Requirements

Several requirements were defined that the output data generated by the air traffic model had to meet:

- Location-dependent requirements of the output data: In order not to increase the modeling efforts untenably high and to keep the required computation power reasonable, the local extension of the model was limited to the North Atlantic within the context of this work. The simulated area was divided into discrete sectors of equal size in order to determine air traffic density for the airborne communication network simulations. Modeling the vertical separation of the simulated aircraft, i.e., an assignment of a specific flight altitude to an aircraft was not realized here.
- Time-dependent requirements of the output data: for the purpose of this study, a representative traffic day (i.e., 24 hours) was simulated with a time interval of

15 minutes, both for the simulation of the status quo and the future situation.

- Extensibility requirement: The model was designed in a way that would enable a future extension to simulate air traffic worldwide.

2.2. Modeling Approach: Status Quo Simulation

In this section, an overview of the general modeling method, developed in order to meet the requirements defined for this study (cf. previous section), is provided. The characteristics of the input and output data used for the simulation of the status quo traffic situation are also explained in more detail.

2.2.1. Input Data

2.2.1.1. OAG Flight Schedules Database

The most important input data for the air traffic model is provided by the OAG flight schedules database which, in the case at hand, contains data of all scheduled commercial flight operations of the year of 2008, i.e., day of flight operation, operating aircraft type, departure and destination airport, date of departure and arrival, time of departure and arrival, available number of seats and freight capacity, and further data [12]. We chose a workday (Tuesday, June 17, 2008) to be the representative day for the status quo simulation. The relevant OAG data columns used for this study are shown in TAB. 1.

TAB. 1: Relevant OAG flight schedules data.

Data	OAG Descriptor
Airline IATA Code	CARRIER 1
Flight Number	FLIGHTNO1
Departure Airport	DEPAIRPORT
Arrival Airport	ARRAIRPORT
Local Departure Time	LOCALDEPTIME
Local Arrival Time	LOCALARRTIME
Flight Time	FLYINGTIME
Aircraft Type	GENERALAC
Weekday of departure	LOCALDAYSOFOF

In order to extract the relevant OAG data from the database, a query was implemented as follows:

- Select all flights operating between the OAG regions North America (OAG: NA1) and Europe (OAG: EU1, EU2), and the Middle East (OAG: ME1), respectively.
- Only select aircraft types of the OAG aircraft categories JW (Wide-body jet aircraft) and JN (Narrow-body jet aircraft).
- Only select flights that either depart at their origin airport or arrive at their destination airport on June 17, 2008 (UTC, universal time coordinated).
- Do not consider flight operations performed by cargo aircraft (e.g. Boeing 747-400F).

With this query, a data file was created that directly serves as input for a Matlab-based air traffic model. The file contains 2,104 single flight events for the status quo simulation.

Note that no air traffic routing information is provided by the OAG database. That is why a method had to be developed to simulate the trajectory that an aircraft takes on its way from its departure to its destination airport. The routing method is explained in section 2.2.2.

2.2.1.2. Aircraft Performance Data

In the context of this study, aircraft performance data is required in particular to determine the speed of an aircraft at cruise flight conditions. This parameter strongly affects the position of the simulated aircraft over time. We assume that all aircraft are at cruise state when entering and exiting the North Atlantic airspace that is simulated in the air traffic model.

TAB. 2: Aircraft types considered in the air traffic model.

OAG Name	BADA Name	Aircraft Type
310	A310	Airbus A310
32S	A320	Airbus A320 series
330	A333	Airbus A330
340	A343	Airbus A340
737	B733	Boeing 737
747	B744	Boeing 747
74M	B744	Boeing 747 mixed config
757	B753	Boeing 757
767	B763	Boeing 767
777	B773	Boeing 777
M11	MD11	Boeing MD-11
TU5	T154	Tupolev TU 154

Here, the cruise speed data of all considered aircraft types (cf. TAB. 2) is derived from Eurocontrol's Base of Aircraft Data (BADA, [13]). The true airspeed information provided in the BADA performance file for cruise flight at flight level 350 (35,000 ft.) is used and wind effects are ignored (i.e., true airspeed = ground speed).

2.2.1.3. Airport Information

Information with regard to the geographical location of each airport contained in the relevant OAG data is required in order to generate the trajectory of each simulated flight (cf. section 2.2.2). Therefore, a data file was created that contains the coordinates of all relevant airports.

Since the time zone of the air traffic model is generally set to UTC, but the OAG departure and arrival information of each flight is given at local time, the airport information file additionally contains data for each airport concerning the relative time offset between an airport and UTC.

2.2.1.4. North Atlantic Tracks (NAT)

When civil aircraft cross the North Atlantic Ocean, they usually fly on predefined air routes called the North Atlantic Tracks (NAT). These airways are defined by the air traffic control authorities. There are multiple NATs destined for eastbound flights crossing the North Atlantic from west to east and also for westbound flights [14]. The westbound NATs are denominated A, B, ... F and the eastbound routes U, V, ... Z (both from northern to southern NAT routes). Each NAT contains an entry and an exit point that geographically define the beginning and the end of the NAT, respectively. In addition, the NATs include several waypoints in between the entry and the exit points.

Air traffic control generally approves certain NATs for flight operations as a function of the current weather and traffic situation. Yet, the final decision which NAT to take is made by the flight crew of each aircraft. This circumstance makes it difficult to simulate real flight trajectories as weather simulation is not implemented in the air traffic model of this study.

The geographical position information of each of the twelve NATs is derived from aeronautical navigation charts used for real flight operations and is contained in a file that serves as input for the definition of the trajectories of the simulated flights.

2.2.2. Time-Dependent Aircraft Localization

In order to be able to identify the current position of each simulated aircraft at any moment during the considered period of time, two vectors are generated that contain the time-dependent geographical coordinates of the aircraft (one for the latitudinal and one for the longitudinal position data). As mentioned before, altitude information is not included in the current version of the model. The air traffic model is time-discretized into intervals of one minute. In order to be able to consider all flights operating on June 17, 2008, the two position vectors are composed by default of 4,320 elements each. This is due to the fact that flights departing on June 16 and flights arriving on June 18 must be considered as well since they may operate overnight or from one day to another.

Until the moment when the aircraft is scheduled to depart from its origin airport according to the OAG data, the coordinates are set to match the coordinates of this airport. Determining the time-dependent aircraft position between the scheduled departure and arrival time is done as follows: the period of time between the departure and arrival time is considered as the entire travel time of the aircraft including all on-ground and in-flight procedures. We name this time t_{TOTAL} . In addition, the departure time t_{DEP} and t_{ARR} are known from the OAG data.

$$(1) \quad t_1 + t_2 = t_{TOTAL} - t_{NAT}$$

In this study, due to lack of data of real flight records, the ratio between the time t_1 and the distance d_1 the aircraft travels from its origin airport to the NAT entry point is assumed equal to the ratio between the sum of t_1 and t_2 and the sum of the distances d_1 and d_2 , where d_2 is the distance traveled between the NAT exit point and the destination airport:

$$(2) \quad \frac{t_1}{d_1} = \frac{t_1 + t_2}{d_1 + d_2}$$

Note that here, d_1 and d_2 are always defined as the shortest distances (i.e., the great circle distances) between the origin airport and an NAT entry point in the case of d_1 and between an NAT exit point and the destination airport in the case of d_2 . The equivalent is applied to t_2 :

$$(3) \quad \frac{t_2}{d_2} = \frac{t_1 + t_2}{d_1 + d_2}$$

The total distance traveled is thus

$$(4) \quad d_{TOTAL} = d_1 + d_{NAT} + d_2$$

We examined this assumption by inspecting the resulting travel speeds v_1 and v_2 of the aircraft on the travel segments d_1 and d_2 by calculating

$$(5) \quad v_1 = v_2 = \frac{d_1}{t_1} = \frac{d_2}{t_2}$$

Tab. 3 shows two example flights to illustrate the impact of the flight route on the values of v_1 and v_2 .

TAB. 3: SEGMENT SPEEDS V_1 AND V_2 OF TWO EXAMPLE FLIGHTS.

Flight	V_{NAT}	$V_1 = V_2$
AA136 LAX-LHR	484 kts	479 kts
AA100 JFK-LHR	484 kts	358 kts

Flight AA136 is serving the route between Los Angeles (LAX) and London Heathrow (LHR) while flight AA100 is operating between New York (JFK) and London Heathrow (LHR), both with Boeing 777 aircraft (i.e., V_{NAT} is the same for both flights). However, the important difference between those two flights is the fact that in the case of flight AA100, d_1 is much shorter compared to flight AA136 (because New York is much closer to an NAT entry point than Los Angeles) while d_2 has approximately the same value for both flights. That is why on-ground operations at the origin airport as well as climb procedures with comparatively low travel speeds relative to V_{NAT} are affecting v_1 much more strongly and thus lower its value. Since the values of v_1 and v_2 seemed reasonable, we considered the assumption of Eq. (2) as adequate with regard to the aircraft speed modeling.

In order to locate the aircraft above the North Atlantic with a suitable degree of precision and with regard to the airborne network modeling approach, we segmented the considered area of the air traffic model into 2,160 sectors; see Figure 1 for illustration. Each segment is positioned between one degree of latitude and its neighbor. Thus, it has a side length of 1°, i.e., 111.2 km. At the time of writing, the available algorithm generates rhombi of corresponding side length, as opposed to a projection with near distance accuracy. Strictly speaking it is only suitable for geographic areas of very limited extent, but we chose to accept resulting inaccuracies for the time being. The position of a simulated aircraft within a segment is not taken into account: from the perspective of the air traffic model, the aircraft is either positioned inside or outside this segment. The latitudinal extension of the considered area is set between 25° and 65°N. The longitudinal extension of one segment is equally set to 111.2 km. 54 divisions are located between 23° and 82°E.

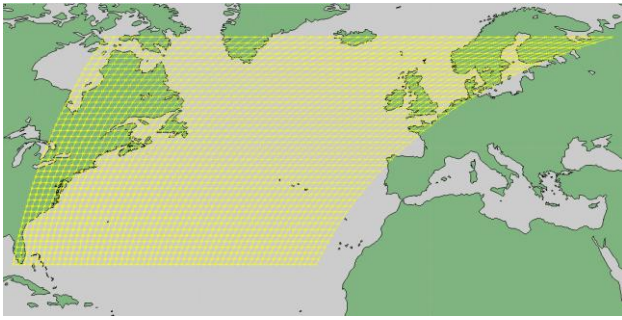


Figure 1: Segmentation of the modeled airspace.

A major issue in modeling the North Atlantic air traffic is created by the assignment of the flight operations to the NATs. As mentioned before, in reality, this decision is made by air traffic control and the cockpit crew, and heavily depends on the current meteorological conditions. It is thus obvious that several assumptions had to be made when assigning the simulated flights to the NATs.

The first assumption is that the pilots would always try to fly on the shortest possible route (i.e., the route that matches the great circle connection best). This assumption by itself does not perfectly reflect reality since meteorological phenomena (wind in particular) influence the pilots' decision, but are not taken into account in this study. In addition to that (and as a consequence of the first assumption), the latitudinal position of the departure airport is assumed to be the main criterion for choosing an NAT. TAB. 4 illustrates how this assumption was implemented. Note that the westbound NATs are denominated A ... F and the eastbound routes U ... Z.

TAB. 4: Assignment of NATs to departure airport.

Latitudinal Location of the departure airport	Assigned NAT
> 60°	A
55° - 60°	B
50° - 55°	C
45° - 50°	D
40° - 45°	E
< 40°	F
> 50°	U
50° - 45°	V
40° - 45°	W
35° - 40°	X
30° - 35°	Y
< 30°	Z

In addition to that, and in order to reflect reality more closely, flights departing from airports which are longitudinally located west of 100°W or east of 30°E, are assigned to NAT A or NAT U, respectively (i.e., the most northern NATs).

2.2.3. Output Data

The modeling approach to aircraft localization and traffic density calculation explained in section 2.2.2 was implemented using Matlab.

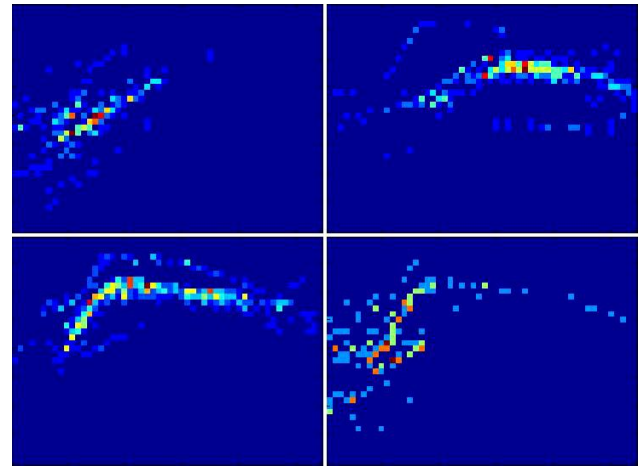


Figure 2: Normalized calculated aircraft densities at roughly 0h, 8h, 16h, and 24h UTC.

For each preselected moment of the simulation period, the tool in the case at hand generates a matrix with 40 lines and 54 columns, representing the simulated airspace above the North Atlantic. The matrices can further be processed using any kind of spreadsheet processing software e.g. for visualizing the time-dependent amount of aircraft passing a certain sector within a certain period of time. Four representative plots of the calculated aircraft density are shown for illustrative purposes in Figure 2.

2.3. Scenario-based Future Evolution

This section describes the approach that was applied to extrapolate the flight schedules data corresponding to the status quo simulation (i.e., Tuesday, June 17, 2008) into a potential future air traffic scenario.

2.3.1. Scenario Planning

The fundamental method behind the approach to the future flight schedules extrapolation that is required within the scope of this study is the scenario planning technique. The core principle of this technique is the methodical development of multiple, alternative, and consistent prospects of the future that contain specific information and quantified data about a predefined future-related research question [15]. Very often, scenarios are developed within a team-based future forecasting project and serve as the basis for corporate strategic decision-making [16]. As such, they mostly contain statements about a future situation on several aggregation levels, starting from a socio-economic, political, and technological top level towards a micro level specific to the individual research purpose.

The future-related work and results presented in this paper are based on the final outcomes of a future forecasting project that was held in the summer of 2012 [17]. The essential outcome of this project that is used as input data for the scope of this paper is formed by the scenario-based, quantified development of the air traffic volume. Three alternative future scenarios had been developed in this future forecasting project. Yet, for the sake of brevity, the results corresponding to one scenario only are considered here (the "Decoupled Powers" scenario, cf. [17]).



Figure 3: Growth rate p.a. of the North-Atlantic air traffic market according to the “Decoupled Powers” scenario [17].

The growth in air traffic volume per year from 2008 until 2050 predicted by the “Decoupled Powers” scenario is shown in Figure 3. Note that only the growth rate for the North Atlantic commercial air traffic market is depicted in this figure (see also [18]).

2.3.2. Future Extrapolation Method

With the scenario-specific future growth rates of air traffic available (Figure 3), a method to predict the related number of aircraft operating above the North Atlantic was developed.

A general problem that occurs when predicting the future air traffic volume and the corresponding number of operating aircraft is the question of aircraft size versus flight frequency [19]: in order to adapt passenger and air cargo capacity to a growing (or shrinking) market, an airline can either

- a) increase (or decrease) the number of operating aircraft belonging to the airline fleet (i.e., increase/decrease the number of flights offered),
- b) or increase (or decrease) the transport capacity of each aircraft of the fleet.
- c) Of course, a combination of both preceding measures is also possible.

In the case of a growing air traffic market, measure a) will increase an airline’s flexibility towards market volatility and better satisfy customer needs with regard to the travel options offered whereas measure b) will reduce operating costs per passenger. Thus, the question of how an airline adapts to a changing market size cannot be answered in a generally applicable way.

In the current version of the air traffic model presented in this paper, the air traffic growth (Figure 2) is assumed to be covered purely by an appropriately rising number of operating aircraft (measure a)). In addition, the modeled fleet operating above the North Atlantic is split into five specific aircraft clusters. This enables a more specific extrapolation process of the fleet. Note that the data related to the future fleet size and structure is derived from the dynamic fleet model presented by Randt [20].

TAB. 5 depicts the scenario-specific growth factors of the North Atlantic fleet for each aircraft cluster from 2008 till 2020 and 2035, respectively. Note that aircraft clusters 3, 4, 5, and 6 are not considered here because they are either representing cargo aircraft or they are not operated above the North Atlantic.

TAB. 5: Growth factors underlying the scenario-specific future fleet extrapolation. Data and fleet extrapolation method based on Randt [20].

A/C Cluster	A/C Example	Growth Factor 2008-2020	Growth Factor 2008-2035
1	Boeing MD-11	1.83	3.33
2	Boeing 747	1.43	2.16
7	Boeing 767	1.37	2.09
8	Airbus A340	1.45	2.39
9	Airbus A320	5.6	14.2

The future flight schedules corresponding to the future fleet are generated on the basis of the flight schedules of 2008 (cf. section 2.2.1.1). The flights operated by the simulated aircraft (cf. TAB. 2) in 2008 are increased in frequency corresponding to the increase of the number operating aircraft in 2020 and 2035, respectively.

3. NETWORK DATA TRAFFIC MODEL

3.1. Per-Aircraft Capacity Demand

The bitrate capacity demand per aircraft depends primarily on the number of passengers which actively use wireless services. The approach outlined in [6] was followed, which describes capacity modeling based on the ETSI internet model. Furthermore, historical web-page statistics [21] were exploited in order to estimate capacity demand, with regard to the situation outlined in [6] and for future extrapolation. Streaming services, including on-demand video and audio, were accounted for by modifying the model accordingly, using statistically generated constant-bitrate streams of variable bitrate respectively length for individual users. Here, Pareto-distributed bitrates and an S-curve like evolution of mean bitrates to a maximum bitrate of 10 Mb/s were assumed (i.e., it was assumed that the capacity requirements for streaming video will saturate within a certain time-frame due to the sensory limitations of human spectators). The temporal statistics which describe the usage patterns were adapted from [6] and may be revised in future iterations of the prognosis. In addition to that, a mean length of 30 minutes was assumed for streaming media; i.e., the results are based on certain assumptions that were deemed plausible at the time of writing due to lack of real-world values for certain statistical parameters.

The cumulative distribution functions for bitrate capacity requirements are shown for a 300-PAX aircraft in Figure 4, assuming that 60% of passengers use mobile services like web browsing, email, streaming audio and video services with intermittent periods of idleness. In Figure 5, the bitrate percentiles are shown as function of year. According to the model, a bitrate capacity of 2.9 Mb/s is sufficient 99% of the time for the year 2008. By 2020, considering internet growth, this figure increases to 89 Mb/s and reaches 735 Mb/s in 2035. The mean bitrates are somewhat lower at 1.7 Mb/s in 2008, 43 Mb/s in 2020 and 312 Mb/s in 2035.

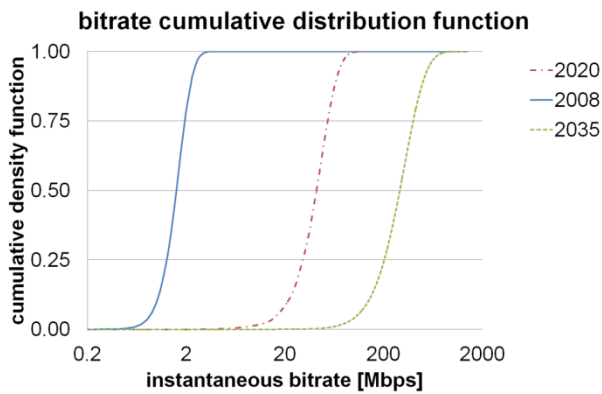


Figure 4: Calculated data traffic CDF for 180 PAX assuming intermittent mobile service use (browsing, streaming audio/video) as function of year.

3.2. Traffic Density-Based Capacity Modeling Approach

In an approach to model network traffic, the air traffic density in the predefined, 2-dimensional grid projection of the North Atlantic corridor is considered as outlined in section 2 (approving of its flaws). HAPs are assumed to be situated above on-shore ground access stations, and are placed along the coastal areas (round “dots”, Figure 6).

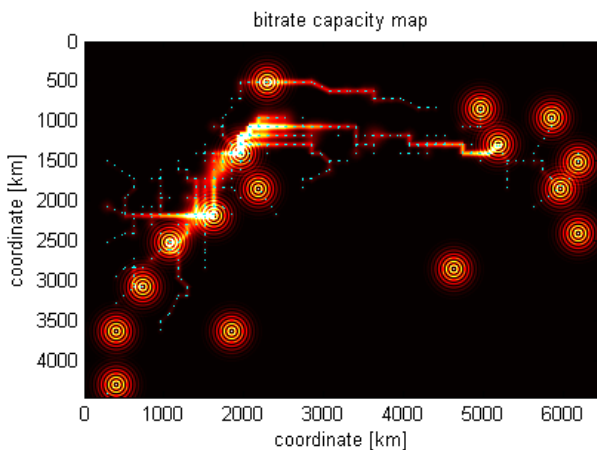


Figure 6: HAPs placement for network simulations along the coasts and islands (modulated “dots”). Representative aircraft density (diffuse “glow”), and individual links with generated traffic are indicated.

Each of the enroute aircraft which participates in the network generates data traffic demand, which is modeled as mean bitrate capacity according to the adapted ETSI model. Here only the “uplink” traffic (i.e., data traffic to the aircraft) is considered. Traffic is routed through the network in a multi-hop fashion to the nearest reachable ground station. It may be that individual aircraft cannot participate in the network due to link range limitations. Capacity demands of individual aircraft are summed up to determine the total bandwidth of each individual, air-to-air link (i.e., transmission “span”) in the ad hoc network.

3.3. Route Finding Methodology

In order to generate routing paths which are viable for a hybrid photonic network, a three-step approach using code written in MATLAB is currently followed:

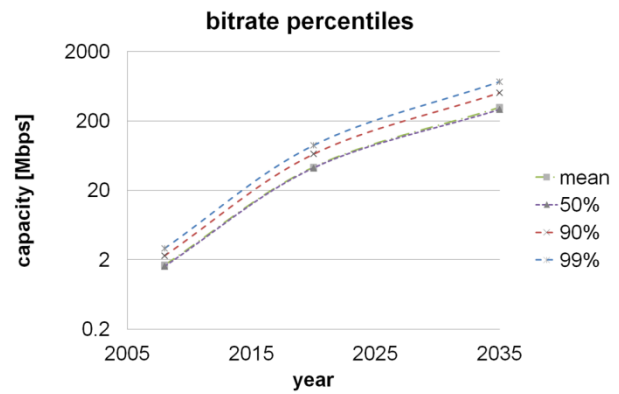


Figure 5: Mean bitrate and percentiles of cumulative distribution function for 180 as function of year according to the adapted ETSI internet traffic model used (lines are guides to the eye).

First the link spans between all communicating entities are represented as a matrix, and the viable ones are extracted using the criterion of maximum link range. The span length is determined geometrically and is later considered as a cost factor for the route finding algorithm. The maximum link range and cost factor can be set individually for aircraft-to-aircraft links and for aircraft-to-HAP links. Next, the network is set up with the remaining spans. The general idea was to minimize the amount of individual connections in the network while providing access to the nearest HAP station; thus an implementation of Prim’s minimum spanning tree (MST) algorithm [22] is used to generate a MST for each HAP, consisting of a set of spans each. The sets of spans are then combined among all ground stations to generate a unified set. Finally, the individual link-paths from HAPs to aircraft are determined from the unified set for each aircraft, using a Matlab implementation of Dijkstra’s shortest path algorithm [23].

3.4. Bitrate Capacity Estimation

In order to calculate the capacity requirement for each span, the aircraft-generated bitrates are determined for the individual paths and then summed up for each individual span. Currently, the same mean bitrate requirement is taken for all aircraft and deviations from this assumption (cf. Figure 4) is expected to be averaged out statistically to a large degree.

4. RESULTS

The model can be used to generate a number of statistics concerning the airborne network. In the following, three important network characteristics are presented: The number of participating aircraft and the maximum backbone capacity in the network as function of the time of day measured in UTC, and capacity-distance statistics summated over 24 hours in 15 minute intervals.

The evolution of network statistics is presented according to the scenario described in section 2, comparing the initial year of 2008 with the scenario-based prognoses for the years 2020 and 2035.

4.1. Connectivity as function of Time

The number of participating aircraft, i.e., the connectivity, remains above 94% at all times throughout the day with the HAP placement shown in Figure 6 (see Figure 7). In the future scenario model, the figure *worsens*

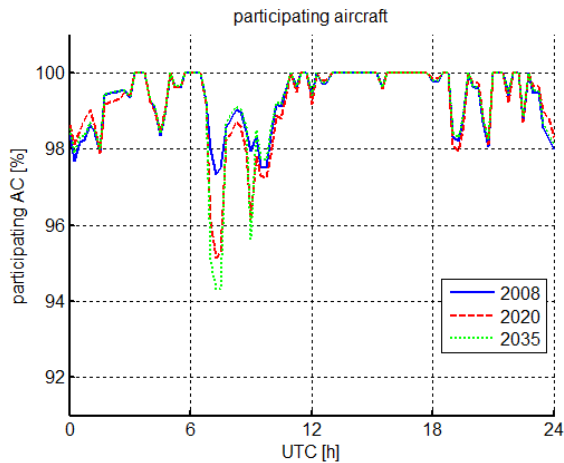


Figure 7: Connectivity as function of time (UTC).

unexpectedly, although the air traffic density *increases*. The reason lies in the first iteration of the scenario-based model, which generates future air-traffic simply by multiplying existing flights. In effect, certain flights fly concurrently and increase air traffic density locally, which may lead to larger drops in the figure when these sectors are cut off from the network. In the next iteration, improved flight scheduling is planned for, which also takes take-off and landing times statistics into account. By strategic placement of additional HAPs, this connectivity figure could be increased in the network model.

4.2. Maximum Backbone Traffic over Time

There is a variation in the capacity requirement of about an order of magnitude, as can be seen in Figure 8. The maximum bitrate capacity in the network varies between around 50 Mb/s and 550 Mb/s in the simulation for 2008. In 2020, the magnitude varies between about 2 and 20 Gb/s, whereas it increases to between about 20 and 200 Gb/s in the prognosis for 2035.

As the route finding algorithm was optimized in order to minimize both branching and overall path distance, the variation in maximum load might be reduced by employing a different path finding strategy, for example by diversity routing mechanisms as outlined in [1]. Nonetheless, the results show that the desired bandwidth capacity approaches the Tb/s-range in 2035 according to the model. This is comparable to what is achieved in contemporary multimode fiber transmission research [24], and moderate when compared to record single-mode fiber transmission [25]; notwithstanding communication channel considerations. Shorter range, free-space optical communication links with Tb/s-capacity have also been demonstrated in the laboratory [26].

4.3. Capacity-Distance Statistics

Over the 24-hour simulation time frame, a two-dimensional bitrate-distance histogram for all link spans was generated for each considered year, see Figure 9 (note the logarithmic scale for the number of links).

A number of interesting properties are observed: In the plot, fragmentation can be seen which is due to the decision to model air traffic density on a 60-Nm grid. The maximum range limitation leads to a discrete number of distances within the statistics. Moreover, most spans are short (111.2 km) with a high dynamic range in capacity

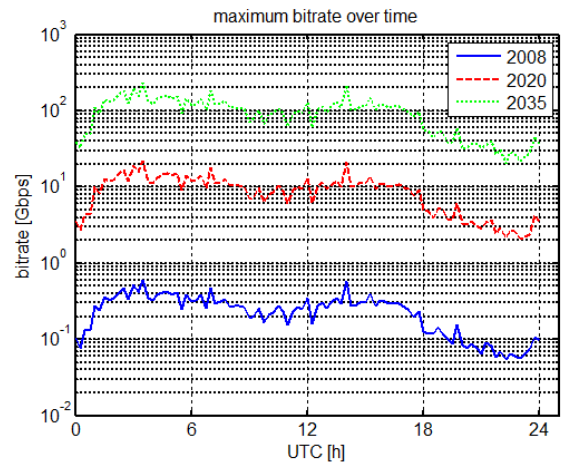


Figure 8: Maximum backbone (i.e., transmission span) traffic in the airborne network over time (UTC).

demand, whereas long-distance links show much reduced capacity requirements. These results are supportive to the initial claim that a high local aircraft density results in a larger capacity requirement while offering the benefit of shorter spans, whereas a lower aircraft density increases inter-aircraft span lengths while requiring less capacity.

This result is well received, because the capacity of free-space communication links drops with communication distance (cf. exemplary curves in Figure 9, right) and free-space optical links have been demonstrated with comparable ranges in less favorable circumstances (i.e., near ground or air-to-ground links) [27] [28]. Moreover, according to the plot, the aircraft density seems high enough to enable agile networking in case of weather-induced outages, infrastructure limitations or other compromising factors.

5. DISCUSSION AND CONCLUSIONS

5.1. Scenario-Based Evolution and Future Prospects

In the first iteration of the model, available flight plan data of 2008 are used to define the status quo in air traffic and extrapolate into the future according to the described scenario process. Though additional flights are added to the flight plan in a defined way according to the expected growth on discrete routes, flight scheduling is not yet done in a comprehensive way. This means that the spatial and temporal structure of the simulated network does not yet evolve as desired. However, the impact on the calculated communication capacity requirements is expected to be tolerable.

As of now, the focus is on a single scenario for the sake of brevity and with regard to the identified shortcomings in the current iteration of the modeling. Shortcomings will be addressed and different scenarios will be considered in future work.

5.2. Weather Impact

In the current state of modeling, the impact of weather on air traffic and on the telecommunication links is ignored. It is planned that weather will be considered for certain aspects of the simulation environment. Naturally, weather plays a role in the choice of flight routes. With regard to telecommunication, weather is one main obstacle with

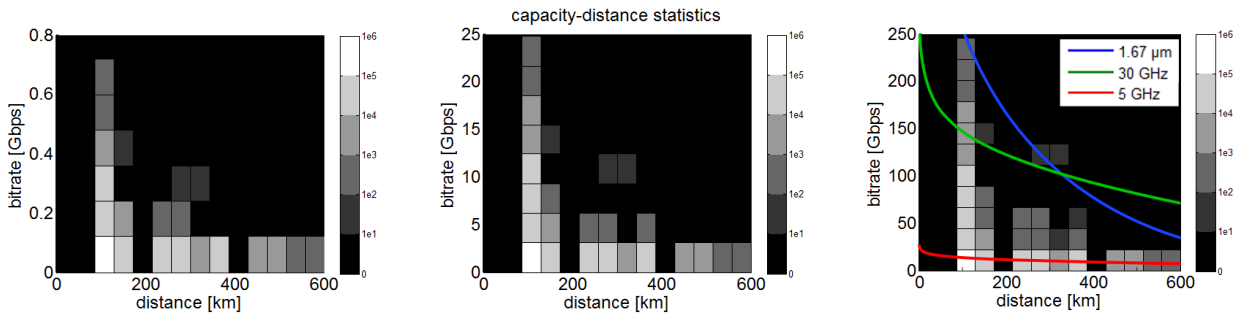


Figure 9: Bitrate-distance statistics over 24 hours for 2008, 2020 and 2035. For comparison, calculated capacity-range curves for transmission at IR, 5-GHz, and 30-GHz frequencies are shown for 2035, based on a simple model and assuming isotropic atmospheric conditions at 9 km altitude (cf. [3]). Modulation bandwidths of 40, 10 and 1 GHz were assumed for the IR, 30 GHz and 5 GHz link, respectively.

regard to wide-spread employment of optical free-space links. The occurrence of aerosols, e.g. in the form of high altitude clouds must be understood for comprehensive studies of airborne laser-based communication networks. Moreover, sky cover statistics play an important role with regard to the placement and density of HAP access points and corresponding ground stations [29].

5.3. HAP Placement

In the current modeling effort, HAPs are placed along the coasts and islands of the North Atlantic with roughly equidistant spacing. As mentioned before, weather statistics have not been taken into account at the time and the placement has not been optimized with regard to optimizing connectivity. Also, the possibility for the installation of ground terminals with sufficient capacity and access to broadband communication lines must be considered at the chosen locations. From a technical point of view, mountaintops would be ideal for the placement of optical telescopes intended for airborne network access points, whereas from an infrastructure view, major airports may be obvious locations for the placement of such terminals with corresponding HAP operation centers.

5.4. Networking Capability Requirements

The branching statistics of the network simulation, employing the described route finding methodology, revealed that a maximum (but low) amount of sectors requires 4 communication branches in order to set up the network (Figure 10). A moderate amount of sectors requires 3 branches, whereas the majority of sectors only channels network traffic via two (“input–output”) terminals. This behavior is attributed to the pre-defined clustering of aircraft to a limited number of sectors. In the conception phase of the hybrid RF-photonic network concept it was deemed plausible that 2 photonic communication terminals per aircraft would be the minimum requirement under the assumption of a serial network topology [3]. Inspection of the network reveals that often, a continuous link with extremely high load to the ground is formed in the network, whereas the branching connections require much reduced capacity. In principle, a 2-terminal photonic backbone architecture might be sufficient to realize a broadband network of large reach most of the time, while the shorter and less bandwidth-hungry branches might be served purely with RF-links. This aspect must be investigated further, especially with regard to interference potentials (RF) and utilization factors of expensive technology (FSO). Therefore, further work is planned to show whether it is possible to set up a hybrid network

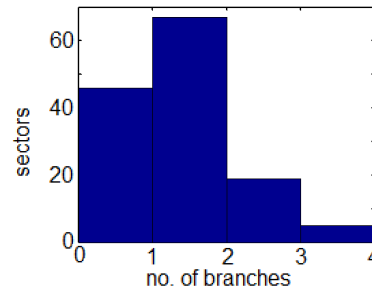


Figure 10: Representative branching statistics.

under the assumption that only certain classes of aircraft (i.e., the largest ones on certain routes) have photonic capability, while the rest hook up to the network with RF-technology, in a cellular-network-like fashion.

5.5. Conclusions

MATLAB models for air traffic simulations along the North Atlantic corridor were developed according to status quo data and future scenarios, for aeronautical communication capacity demand as function of passenger count and usage statistics, and for airborne network simulations. Results show that in 2020, such a network would require a backbone capacity on the order of 20 Gbps, whereas in 2035, this figure increases to about 200 Gbps.

The network model was not driven by capacity limitations but by simplifying the network infrastructure, with regard to the proposed network architecture. Thus, the maximum communication capacity requirement varies by about an order of magnitude over time, with a large spread observed when all link spans are compared to another. The route finding algorithm can be modified in order to allow for more flexible routing and better load distribution in order to reduce maximum capacity demand.

Capacity-distance statistics indicate that capacity demand is reduced for longer spans, which is a favorable result with regard to channel capacity. The maximum capacity requirement for individual spans of hundreds of Gb/s in 2035 is technologically achievable by wavelength multiplexing techniques already today, but is yet to be demonstrated in a complex environment like the airborne networking scenario, with the challenging atmospheric channel. The design and integration of airborne optical terminals with sufficient range and coping strategies for atmospheric turbulence mitigation poses a challenge, and will have to be addressed in further research.

REFERENCES

- [1] D. Medina, F. Hoffmann, S. Ayaz, and C.-H. Rokitzky, "Feasibility of an Aeronautical Mobile Ad Hoc Network Over the North Atlantic Corridor," in *5th Annual IEEE Communications Society Conference on Sensor, Mesh and Ad Hoc Communications and Networks*, San Francisco, CA, 2008, pp. 109-116.
- [2] D. Medina and F. Hoffmann, "The Airborne Internet," in *Future Aeronautical Communications*, InTech, 2011, ch. 17, pp. 349-374.
- [3] K.-D. Büchter, A. Reinhold, G. Stenz, and A. Sizmann, "Drivers and Elements of Future Airborne Communication Networks," in *Deutscher Luft- und Raumfahrtkongress*, Berlin, Germany, 2012.
- [4] P. Bishop, A. Hines, and T. Collins, "The current state of scenario development: an overview of techniques," *Foresight-The journal of future studies, strategic thinking and policy*, vol. 9, no. 1, pp. 5-25, 2007.
- [5] M. Kavehrad, Z. Hajjarian, and A. Enteshari, "Energy-efficient broadband data communications using white LEDs on aircraft powerlines," in *IEEE Integrated Communications, Navigation and Surveillance Conference*, Bethesda, MD, 2008, pp. 1-8.
- [6] P. Unger and L. Battaglia, "Dynamic Behavior of AirCom Internet Users on Long-Haul North Atlantic Flights," in *IEEE International Conference on Communications*, Vol. 7, Paris, France, 2004, pp. 3947-3952.
- [7] P. Valtr and P. Pechač, "Tropospheric Refraction Modeling Using Ray-Tracing and Parabolic Equation," *Radioengineering Journal*, vol. 14, no. 4, pp. 98-104, 2005.
- [8] K.-D. Büchter and A. Sizmann, "Feasibility of High-Speed Transparent Photonic Links in Airborne Free-Space Optical Communication," in *IEEE Avionics, Fiber-Optics and Photonics Conference (Accepted)*, San Diego, CA, 2013, pp. 1-2.
- [9] S. Gordon and R. Neufville, "Design of air transportation networks," *Transportation Research Journal*, vol. 7, no. 3, pp. 207-222, 1973.
- [10] H. Matsumoto, "International air network structures and air traffic density of world cities," *Transportation Research*, vol. E, pp. 269-282, 2007.
- [11] E. Salaün, M. Gariel, A. E. Vela, and E. Feron, "Aircraft Proximity Maps Based on Data-Driven Flow Modeling," *Journal of Guidance, Control and Dynamics*, vol. 35, no. 2, 2012.
- [12] OAG Aviation Solutions. (2008) Official Airline Guide Flight Schedules Database June 2008.
- [13] "BADA: Base of Aircraft Data Aircraft Performance Modeling Report: EEC Technical/Scientific Report No. 2009-009," Eurocontrol Experimental Centre (Ed.), Brétigny-sur-Orge, France, 2009.
- [14] "North Atlantic Operations and Airspace Manuel - Edition 2012," ICAO, NAT Doc 007 2012.
- [15] U. Pillkahn, , John Wiley, Ed. Weinheim, Chichester: Wiley-VCH, 2007.
- [16] J. Verity, "Scenario planning as a strategy technique," *European Business Journal*, vol. 15, no. 4, pp. 185-195, 2003.
- [17] N. P. Randt, Ch. Jeßberger, K. O. Plötner, and A. Becker, "Air Traffic Growth, Energy, and the Environment 2040: Drivers, Challenges and Opportunities for Aviation," in *17th Conference of the Air Transport Research Society*, Bergamo, Italy, 2013.
- [18] N. Randt and G. Oettl, "Applied Scenario Planning as a Basis for the Assessment of Future Aircraft Technologies," in *Deutscher Luft- und Raumfahrtkongress*, Stuttgart, Germany, 2013.
- [19] V. Pai, "On the factors that affect airline flight frequency and aircraft size," *Journal of Air Transport Management*, vol. 16, no. 4, pp. 169-177, 2010.
- [20] N. P. Randt, "Foundations of a Technology Assessment Technique Using a Scenario-Based Fleet System Dynamics Model," in *13th AIAA Aviation Technology, Integration, and Operations (ATIO) Conference*, Los Angeles, CA, 2013.
- [21] (2012) Website Optimization. [Online]. <http://www.websiteoptimization.com/speed/tweak/average-web-page/>
- [22] A. Greenbaum. (2007) Matlab: Prim minimum spanning tree algorithm. http://www.math.washington.edu/~greenbau/Math_381/programs/prim.m.
- [23] W. Xiaodong and M. Shirazipour. (2009) Matlab: Dijkstra shortest path algorithm. <http://www.mathworks.com/matlabcentral/fileexchange/5550-dijkstra-shortest-path-routing>.
- [24] I. Gasulla and J. Capmany, "1 Tb/s-km Multimode fiber link combining WDM transmission and low-linewidth lasers," *Optics Express*, vol. 16, no. 11, pp. 8033-8038, 2008.
- [25] J.-X. Cai et al., "25 Tb/s transmission over 5,530 km using 16QAM at 5.2 b/s/Hz spectral efficiency," *Optics Express*, vol. 21, no. 2, pp. 1555-1560, 2013.
- [26] E. Ciaramella et al., "1.28 Tb/s (32 x 40 Gb/s) Free-Space Optical WDM Transmission System," vol. 21, no. 16, 2009.
- [27] J. Horwath and Ch. Fuchs, "Aircraft to ground unidirectional laser-communications terminal for high-resolution sensors," *SPIE LASE: Lasers and Applications in Science and Engineering*, 2009.
- [28] J. C. Juarez, D. W. Young, J. E. Sluz, J. L. Riggins II, and D. H. Hughes, "Free-space optical channel propagation tests over a 147-km link," in *SPIE Defense, Security, and Sensing. International Society for Optics and Photonics*, 2011, pp. 80380B-80380B.
- [29] J. Horwath, N. Perlot, M. Knapek, and F. Moll, "Experimental verification of optical backhaul links for high-altitude platform networks: Atmospheric turbulence and downlink availability," *International Journal of Satellite Communications and Networking*, vol. 25, pp. 501-528, 2007.